Physica C 507 (2014) 17–21

Contents lists available at ScienceDirect

Physica C

journal homepage: www.elsevier.com/locate/physc

Higher oxidization rate of photo-assisted annealing compared with thermal annealing after $YBa_2Cu_3O_{7-\delta}$ films growth

Guoxing Li [a], Shanwen Li [a], Wei Li [b], Xinsheng Wang [a], Feng Guo [a], Baolin Zhang [a,*], PenChu Chou [a]

[a] State Key Laboratory on Integrated Optoelectronics, College of Electronic Science and Engineering, Jilin University, Changchun 130012, China
[b] National Engineering Research Center for Optoelectronics Devices, Institute of Semiconductors, Chinese Academy of Sciences, Beijing 100083, China

ARTICLE INFO

Article history:
Received 7 May 2014
Received in revised form 17 July 2014
Accepted 9 September 2014
Available online 18 September 2014

Keywords:
REBCO
Annealing
Photo activation
Oxidization

ABSTRACT

In order to study the possible advantage of photo-assisted MOCVD compared with thermal MOCVD during the annealing process after film growth, a piece of *c*-axis oriented $YBa_2Cu_3O_{7-\delta}$ film on Φ1″ $LaAlO_3$ (100) substrate was prepared by photo-assisted MOCVD. It has well in-plane alignment and high critical current density (J_c > 2.5 MA/cm^2, @ 0 T, 77 K, thickness ≈ 430 nm). Small pieces cut from it were annealed by photo-assisted or thermal annealing process to realize deoxidization or oxidization respectively. By monitoring the *c*-axis lattice constant, it was found that oxidization rate of photo-assisted annealing is obviously higher than that of thermal annealing. Inversely, the deoxidization rate of photo-assisted annealing is lower than that of thermal annealing. And a phenomenon that the long-time stable *c*-axis lattice constant is related to the temperature, unrelated to annealing process has been observed. It conforms to the thermodynamic equilibrium which is relative to annealing temperature and oxygen partial pressure, irrespective to whether photo activation or thermal activation.

1. Introduction

$REBa_2Cu_3O_{7-\delta}$ (REBCO, RE = rare earth Y, Dy, Gd, etc.) are charming materials because of their high performance and low refrigeration cost for high temperature superconducting (HTS) applications. Especially films grown on larger area dielectric crystal wafers and long distance flexible metal tapes are forming a huge market refer to microwave applications and electric power applications correspondingly. Researchers have made great success using multiple methods to grow $REBa_2Cu_3O_{7-\delta}$ films such as Metal Organic Chemical Vapor Deposition (MOCVD) [1,2], Thermal Co-evaporation [3,4], Metal Organic Deposition (MOD) [5,6], and Pulse Laser Deposition (PLD) [7,8]. Technical difficulties refer to preparing high performance in large area (or long distance) have been overcome by some advanced institutions. Thus, further improving the preparation efficiency and declining cost should attract the attention of the application researchers and manufacturers.

Photo-assisted processes, such as photo-assisted annealing (rapid isothermal treatment) and photo-assisted film growth techniques [9–12], are widely used in electronic materials processing. Compared with the ordinary heat treatment technology, some benefits were considered as the result of photo activation in photo-assisted process. There have been some reports referring to the well alignment and high-speed growth of superconducting $YBa_2Cu_3O_{7-\delta}$ (YBCO), $GdBa_2Cu_3O_{7-\delta}$ (GdBCO) films by photo-assisted MOCVD [13–15]. But the effect of photo activation during the film thermal treatment after film growth has not been studied. For example the YBCO film growth by photo-assisted MOCVD mentioned in this paper, the thermal treatment time is 85 min from process ***III*** to ***VI*** in Fig. 1. It is 28 times long of film growth time of 3 min for process ***II***. This paper just focused on the effect of photo activation during thermal treatment process after YBCO film growth. Possibly, the results could also inspire the other preparation methods to shorten thermal treatment time.

It is well known that the oxygen content ($7-\delta$) of YBCO can be varied from 6.0 to 7.0 continuously. The oxygen content of YBCO is about 6.0 after growth in high temperature of about 800 °C. Normally, that YBCO was tetragonal and without superconductivity. But, oxygen content can be varied from 6.0 to near 7.0 after the thermal annealing in oxygen atmosphere. In this way, orthorhombic YBCO with superconductivity (critical temperature is about 91 K) could be acquired and $YBa_2Cu_3O_{6.9}$ has been considered to be that with best superconductivity [16–18]. Therefore, oxygen content dependent on annealing time and annealing temperature by photo-assisted annealing or thermal annealing is the key of thermodynamics and kinetics analysis in this study. The following

* Corresponding author. Tel.: +86 431 85168240.
E-mail address: zbl@jlu.edu.cn (B. Zhang).

http://dx.doi.org/10.1016/j.physc.2014.09.003
0921-4534/

problems will be clear: In kinetics, whether photo-assisted annealing processing increases the oxidization rate and deoxidization rate for the YBCO films. In thermodynamics, whether the photo-activation could change the reaction equilibrium and reduce the heat treatment temperature.

2. Experimental

An YBCO film was grown on a Φ1″ $LaAlO_3$ (100) (LAO (100)) substrate by photo-assisted MOCVD at substrate temperature of 810 °C in about 3 min. The system diagram of this system was reported before [19], and the 1″ LAO (100) substrate was placed in the center of a sample holder of 100 mm diameter with 400 r/min revolving. Fig. 1 shows the substrate temperature and oxygen partial pressure changing during the film growth and in-situ heat treatment process. X-ray diffraction (XRD, test instrument: Rigaku Ultima V) two-theta scan and phi scan was employed to evaluate its growth orientation and in-plane alignment. *c*-axis lattice constant of all samples in this paper were calculated by Bragg equation according to XRD-2θ scan patterns.

After above-mentioned growth and in-situ heating treatment, the sample was regarded as fully oxidized YBCO in this study. Its XRD-2θ pattern is shown as red plot in Fig. 2, and its *c*-axis constant was c = 1.168 nm calculated by Bragg equation according to YBCO (005) peak. After measurement of superconducting critical current density (J_c) by mapping analysis of inductive-J_c data (test instrument: THEVA Cryoscan) small pieces cut from half of this sample were used for deoxidization by photo-assisted and thermally annealing study.

The other half was heated in one atm (~0.1 MPa) argon atmosphere up to 780 °C for 2 h by photo-assisted annealing, and then slowly cooled down to room temperature with a speed of 10 °C/min. This sample was regarded as fully deoxidized YBCO in this study. Then, XRD-2θ and XRD phi scan was employed to compare with the fully oxidized YBCO sample. The *c*-axis constant of this fully deoxidized YBCO sample was 1.179 nm calculated by Bragg equation according to YBCO (005) peak in its XRD-2θ pattern shown as blue plot in Fig. 2.

Small pieces cut from this half part were used for oxidation by photo-assisted and thermal annealing study.

For thermally oxidized and deoxidized annealing, a tubular furnace was employed. The heat source in that furnace is a high power resistance wire made of nichrome. Usually, temperature of the resistance wire is a little higher than the target temperature of substrate and with little fluctuation. But it was less than 800 °C according to our monitor during these experiments in this study. For photo-assisted oxidized and deoxidized annealing, five high power halogen tungsten quartz lamps were employed. Those

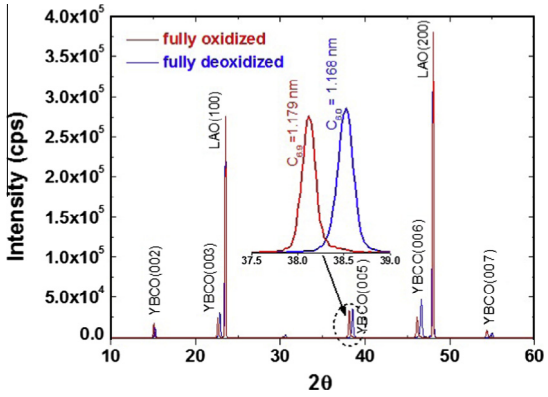

Fig. 2. XRD-2θ patterns of YBCO samples. The red plots belong to half YBCO sample considered as fully oxidized YBCO; the blue plots belong to the other half YBCO sample considered as fully deoxidized YBCO. The inset is enlargement of YBCO (005) peaks. (For interpretation of the references to color in this figure legend, the reader is referred to the web version of this article.)

lamps have been kept above 85% their rated power by adjusting the distance between lamps and substrate to keep them in high color temperature. Based on the theory of blackbody radiation, radiation light from the resistance wire of tubular furnace mainly concentrated in the infrared wavelengths with little visible light. But radiation light from the halogen tungsten quartz lamps mainly concentrated in the visible wavelengths and with a little ultraviolet light and infrared wavelengths. Thus, during thermal annealing process only thermal activation is active, but during photo-assisted annealing processes both thermal activation and photo-activation is active.

For oxidation, small pieces cut from fully deoxidized half sample were annealed by photo-assisted or thermally at 460 °C or 550 °C under an environment of one atm oxygen for 10–120 min. And, for deoxidization, small pieces cut from fully oxidized half sample were annealed at 460 °C and 550 °C under an environment of one atm nitrogen for 10–120 min. During those annealing process, for the sake of minimizing the influences of heating and cooling process, the heating or cooling process was controlled as soon as possible (generally within 5 min).

Obviously, a precise measurement of oxygen content of each YBCO thin film sample is very difficult. But according to the previous report, the *c*-axis length has linear relationship with the oxygen content of YBCO, which is shown as Fig. 3 [17]. Obviously, *c*-axis length of YBCO is also influenced by content proportion of yttrium, barium and copper. Thus an accurate formula which can calculate the oxygen content according to lattice constant *c* cannot be given. But, the small pieces of YBCO in this study were cut from

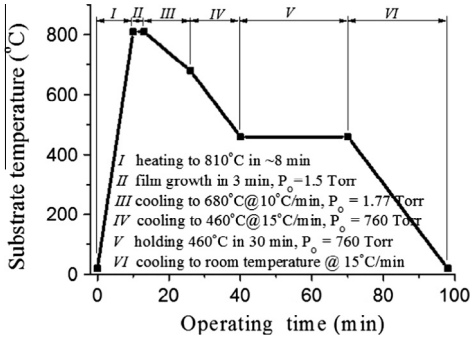

Fig. 1. Substrate temperature and oxygen partial pressure (P_O) changes during the YBCO/LAO film growth and in-situ heat treatment process. It can be divided into six detailed process from ***I*** to ***VI***.

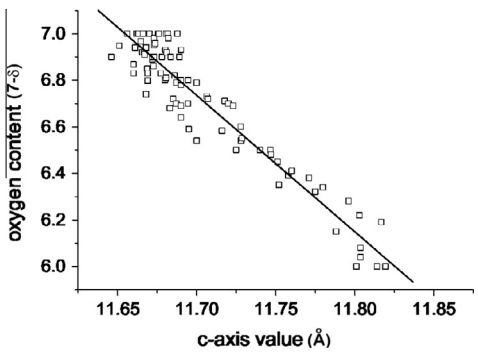

Fig. 3. Oxygen content ($7-\delta$) values as a function of the *c*-axis values obtained from ICSD database. The solid line is the fit of the points [17].